

15. Grafts fixed with Bouin's solution were embedded in paraffin, which was subsequently removed from 5- μ m sections by treatment with xylene. The sections were rehydrated by exposure to a graded series of ethanol solutions, and endogenous peroxidase was quenched with 0.1% H₂O₂ in phosphate-buffered saline (PBS) for 15 min. Nonspecific sites were blocked with 10% goat serum and 0.3% Triton X-100 in PBS for 1 hour, with addition of free avidin to block endogenous biotin followed by incubation for 30 min with free biotin. The sections were then incubated overnight at 4°C with undiluted culture supernatant from pFAS-Foll-transfected Neuro-2a

cells. Fas-Fc binding was detected by sequential application of biotin-conjugated goat antibodies to human immunoglobulin (Fc specific), streptavidin-conjugated horseradish peroxidase, and diaminobenzidine substrate solution (Zymed, San Francisco, CA). Sections were then counterstained with hematoxylin.

16. Grafts fixed with Bouin's solution were processed for paraffin sectioning. Deparaffinized and rehydrated sections were digested with proteinase K (20 μ g/ml) for 15 min at room temperature, and endogenous peroxidase activity was quenched with 0.1% H₂O₂ in PBS for 15 min. Sections were then incubated with

10% goat serum in PBS for 1 hour, after which the 3'-OH ends of fragmented DNA were labeled by TUNEL with an in situ cell death detection kit (Boehringer Mannheim, Mannheim, Germany). Sections were then counterstained with eosin.

17. Care and use of all animals were in accordance with the guidelines of the animal care committee of the Children's Hospital of Philadelphia. We thank J. M. Templeton Jr. for his support; K. High and S. Surrey for critical review of the manuscript; and S. Nagata for reagents.

23 January 1996; accepted 2 May 1996

Evidence for Physical and Functional Association Between EMB-5 and LIN-12 in *Caenorhabditis elegans*

E. Jane Albert Hubbard, Qu Dong, Iva Greenwald*

The *Caenorhabditis elegans* LIN-12 and GLP-1 proteins are members of the LIN-12/Notch family of receptors for intercellular signals that specify cell fate. Evidence presented here suggests that the intracellular domains of LIN-12 and GLP-1 interact with the *C. elegans* EMB-5 protein and that the *emb-5* gene functions in the same pathway as the *lin-12* and *glp-1* genes. EMB-5 is similar in sequence to a yeast protein that controls chromatin structure. Hence, a direct consequence of LIN-12 or GLP-1 activation may be an alteration of chromatin structure that produces changes in transcriptional activity.

Transmembrane proteins of the LIN-12/Notch family are found throughout the animal kingdom. The *Caenorhabditis elegans* genes *lin-12* and *glp-1* and the *Drosophila* gene *Notch* were first defined by mutations that alter cell fate decisions involving cell-cell interactions (1–3). In vertebrates, *lin-12/Notch* genes are also involved in cell fate decisions (4). It is now generally accepted that LIN-12/Notch proteins function as receptors that are activated by binding ligands of the Delta/Serrate/LAG-2 family (5). The intracellular domain of LIN-12/Notch proteins, and in particular the region encompassing six CDC10/SW16 (ankyrin) motifs, has the intrinsic signal-transducing activity of the intact protein (6). However, there is no known biochemical activity associated with the intracellular domain of LIN-12/Notch proteins. Understanding the downstream consequences of receptor activation therefore requires the identification and characterization of the interacting components involved in *lin-12/Notch*-mediated cell fate decisions.

E. J. A. Hubbard and Q. Dong, Department of Biochemistry and Molecular Biophysics, Columbia University College of Physicians and Surgeons, New York, NY 10032, USA.

I. Greenwald, Department of Biochemistry and Molecular Biophysics and Howard Hughes Medical Institute, Columbia University College of Physicians and Surgeons, New York, NY 10032, USA.

*To whom correspondence should be addressed. E-mail: greenwald@cuccfa.ccc.columbia.edu

One such component, named Su(H) in *Drosophila* and LAG-1 in *C. elegans*, is similar to the mammalian CBF1 transcription factor (7, 8). Genetic studies in *Drosophila* and *C. elegans* have established that Su(H) and LAG-1 are involved in LIN-12/Notch-mediated reception of intercellular signals (7, 9–11). Furthermore, Su(H) interacts physically with the intracellular domain of Notch (10). These findings, along with the observations that the intracellular domains of LIN-12/Notch proteins have intrinsic signal-transducing activity and when expressed alone are localized in the nucleus, have led to models proposing that there is no intervening cascade of second messengers involved in signal transduction initiated by LIN-12/Notch activation. Instead, upon receptor activation, the intracellular domain may influence target gene expression by activating a transcription complex, or it may function as part of a transcription complex (5).

To identify potential components involved in LIN-12/Notch signal transduction, we used the yeast two-hybrid screen (12, 13). A plasmid library of fusions between the GAL4 activation domain (GAD) and *C. elegans* cDNA sequences (14) was screened for interaction with a fusion protein containing the Gal4p DNA binding domain (GBD) and the CDC10/SW16 (ankyrin) motifs of LIN-12 (15). Partial-sequence analysis of candidate clones and

subsequent database searches revealed that two clones, E7 and E16, contain different GAD fusions to EMB-5 sequences (Table 1). E7 and E16 also interact to a comparable extent with a fusion protein containing the corresponding region of GLP-1 fused to GBD (Table 1). This result suggests that the interaction is meaningful, because *lin-12* and *glp-1* are functionally and biochemically interchangeable (9, 16). In contrast, E7 and E16 do not interact with the functionally and structurally unrelated proteins laminin (human) and SNF1 (*Saccharomyces cerevisiae*), or with a functionally unrelated *C. elegans* protein FEM-1 that contains CDC10/SW16 motifs (Table 1).

Table 1. EMB-5 interacts with LIN-12 and GLP-1 in the yeast two-hybrid system. Yeast strain Y153 (13) was sequentially transformed with (i) a plasmid encoding a fusion protein between the Gal4p DNA binding domain (GBD) and another sequence (DNA binding hybrid) and (ii) a plasmid encoding a fusion protein between the Gal4p activation domain (GAD) and another sequence (activation hybrid). A blue colony color in the filter assay indicates that β -galactosidase (β -Gal) activity is present, implying a physical association between the DNA binding and activation domain hybrids as a result of inserted sequences. nd, not done.

DNA binding hybrid*	Activation hybrid†	Colony color	β -Gal activity (Miller units)‡
LIN-12	EMB-5	Blue	4.7 \pm 0.6
GLP-1	EMB-5	Blue	5.3 \pm 0.2
LIN-12	SNF4	White	0.8 \pm 0.6
GLP-1	SNF4	White	0.4 \pm 0.1
SNF1	EMB-5	White	0.6 \pm 0.1
Lamin	EMB-5	White	nd
FEM-1	EMB-5	White	nd
SNF1	SNF4	Blue	28.5 \pm 4.5

*DNA binding hybrids in the pAS1 vector (13) contain sequences fused to GAL4p(1–147). LIN-12 = pASL2, containing LIN-12(940–1320). GLP-1 = pASG2, containing GLP-1(867–1171). pAS-SNF1 was derived from pEE5 (12). pAS-FEM-1 encodes a hybrid containing the CDC10-SW16 motifs of FEM-1 (26). †EMB-5 activation domain hybrids in the pACT vector contain sequences fused to GAL4p(768–881) (13). For EMB-5, the data are from the E7 clone, which contains EMB-5(894–1521). Similar results were obtained for the E16 clone, which contains EMB-5(835–1521) (27). The SNF4 clone was pNI12 (12). ‡Miller units are described in (28). The standard deviation is indicated. Each value is the average of four transformants.

Mutant alleles of *emb-5* were identified previously in screens for temperature-sensitive embryonic lethal mutations (17). With the use of these temperature-sensitive alleles, we obtained evidence that the physical interaction implied by the two-hybrid screen is functionally relevant in vivo. We have focused our genetic analysis on two cell fate decisions, the *lin-12*-mediated anchor cell-ventral uterine precursor cell (AC-VU) decision and the *glp-1*-mediated mitosis-meiosis decision during germline development.

The AC-VU decision occurs during development of the somatic gonad. Two equivalent cells, Z1.ppp and Z4.aaa, interact with each other so that one of these cells becomes the AC and the other becomes a VU (18, 19). When *lin-12* activity is eliminated, both Z1.ppp and Z4.aaa be-

come ACs (the "2 AC defect"), and when *LIN-12* is constitutively activated, as in *lin-12(n302)* mutants, both Z1.ppp and Z4.aaa become VUs (the "0 AC defect") (2). In wild-type hermaphrodites, a stochastic variation in ligand or receptor activity (or both) between Z1.ppp and Z4.aaa appears to be amplified by a feedback mechanism that involves transcriptional control of ligand and receptor expression (19, 20).

When *emb-5* mutants are shifted from the permissive to the restrictive temperature after embryogenesis, they have a single AC, as in the wild type (see below). However, by three different genetic criteria, *emb-5* appears to function in the AC-VU decision. (i) *emb-5* mutations enhance the penetrance of the 2 AC defect of *lin-12* hypomorphs (Table 2). (ii) Reduction of *emb-5* activity lowers the penetrance of the 0 AC defect associated with constitutively active *LIN-12* (Table 2). (iii) The relative amount of *emb-5* activity in Z1.ppp and Z4.aaa, like the relative amount of *lin-12* activity, can bias the AC-VU decision (Fig. 1A). Genetic mosaics in which either Z1.ppp or Z4.aaa had reduced *emb-5* activity

when the other cell was *emb-5(+)* always had a single AC. However, in 22 out of 24 mosaics, the *emb-5* mutant cell became the AC. Thus, a genotypically wild-type cell in the mosaic no longer has a 50% chance of becoming the AC, as it does in a wild-type hermaphrodite. This bias in cell fate choice in genetic mosaics is similar to that seen for genetic mosaics involving *lin-12* (19) and suggests that *emb-5* is involved in specifying the fate of the presumptive VU. Neither *lag-2* (ligand) nor *lin-12* reporter gene expression (20) was grossly affected by reduction of *emb-5* activity, consistent with *emb-5* function downstream of *lin-12* (21).

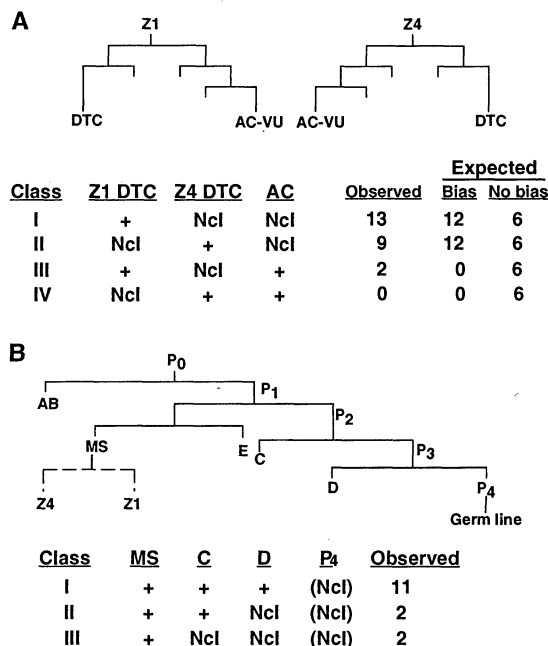
The *emb-5* gene also may function in other *lin-12*-mediated cell fate decisions, such as specification of vulval precursor cells, because *emb-5* can enhance the penetrance of the vulval morphology defect associated with reduced *lin-12* activity (21). However, *emb-5* mutants did not display characteristic *lin-12* (or *glp-1*) cell fate transformations after the temperature shift (Table 2). This observation may indicate that the available *emb-5* temperature-sensitive mutations do

Table 2. Reduction of *emb-5* activity lowers *lin-12* activity. Hermaphrodites were scored at 25°C unless otherwise indicated. Animals scored at 25°C were synchronized and shifted from 15°C during late embryogenesis or the early L1 stage. Pairs of corresponding genotypes with and without *emb-5* were shifted at the same time. Cell fate transformations were scored by Nomarski microscopy with the criteria described in (2). The number (n) in parentheses is the number of individuals examined. *emb-5(hc61)* and *emb-5(g65)* are described in (17). We found that the genotype of the published MJ61 strain (17) is actually *emb-5(hc61) lin-12(ar170)*, and for the experiments here, we reisolated *emb-5(hc61)* and *lin-12(ar170)* as single mutants from MJ61 (21). The hypomorphic allele *lin-12(n676n930)* is described in (28), and the ligand-independent hypermorphic allele *lin-12(n302)* is described in (2, 30).

Genotype	2 AC (%) (n)*
emb-5 enhancement of lin-12 alleles	
<i>lin-12(+)</i>	0
<i>lin-12(n676n930)</i>	22 (54)
<i>emb-5(hc61) lin-12(n676n930)</i>	46 (82)
<i>emb-5(g65) lin-12(n676n930)</i>	70 (111)
<i>emb-5(hc61)</i>	0 (66)
<i>emb-5(g65)</i>	0 (119)
<i>lin-12(0)</i>	100
<i>lin-12(ar170)</i>	73 (78)
<i>emb-5(hc61) lin-12(ar170)</i>	100 (33)
<i>emb-5(g65) lin-12(ar170)</i>	92 (75)
<i>lin-12(ar170)</i> (20°C)	27 (75)
<i>emb-5(hc61) lin-12(ar170)</i> (20°C)	70 (66)
<i>emb-5(g65) lin-12(ar170)</i> (20°C)	46 (63)
Genotype†	
	0 AC (%) (n)‡
emb-5(hc61) suppression of a lin-12 allele	
<i>lin-12(n302)/+</i>	59 (47)
<i>emb-5(hc61) lin-12(n302)/</i> <i>emb-5(hc61) lin-12(+)</i>	39 (43)

*Proportion of hermaphrodites having 2 AC, as in a *lin-12(0)* mutant. †Complete genotypes: *lin-12(n302)/unc-32(e189)*; *him-5(e1490)/+* and *emb-5(hc61) lin-12(n302)/emb-5(hc61) unc-32(e189)*; *him-5(e1490)/+*. ‡Proportion of hermaphrodites with a 0 AC-Egl phenotype, as in a *lin-12* hypermorphic (gain-of-function) mutant.

Fig. 1. Genetic mosaics of the *emb-5* gene. Relevant cell lineages are shown (31). Mosaics segregating from *emb-5(g65) ncl-1(e1865) unc-36(e251); sDp3* hermaphrodites raised at 25°C were examined as described below. *sDp3* complements all markers, and *ncl-1* is a cell-autonomous marker for most somatic cells that causes an enlarged nucleolus that can be scored under Nomarski optics (32). The *unc-36* focus of activity is in the ABp lineage (33). (A) Approximately 850 non-Unc L3 hermaphrodites were screened to obtain 24 mosaic individuals that had one Ncl distal tip cell (DTC) and one wild-type (+) distal tip cell, indicating the loss of *sDp3* in the Z1 or Z4 lineage as in (19). The number and Ncl phenotype of the AC of each mosaic was then determined. All mosaic hermaphrodites had one AC. In 22 out of 24 mosaics, the *emb-5* mutant cell became the AC. The two exceptions (class III) may have resulted from an incomplete bias, which might reflect an incomplete requirement for *emb-5* function or residual activity of *emb-5(g65)* at the restrictive temperature. Alternatively, the rare class III mosaics may have resulted from a late loss of *sDp3* within the Z4 lineage. We were unable to ascertain if this was the case because the Ncl phenotype of the gonadal cells descending from Z4.a and Z4.p could not be reliably scored. Control experiments with hermaphrodites of genotype *emb-5(+)* *ncl-1 unc-36; sDp3* have shown that the *ncl-1* and *unc-36* markers do not cause this bias in cell fate choice (19, 21). (B) Sterile non-Unc mosaic hermaphrodites were scored for the Ncl phenotype to ascertain the focus of *emb-5(+)* activity for fertility as described in (3). For the MS, C, and D lineages, Ncl and + indicate evidence for loss or presence (respectively) of the duplication in an entire lineage. The Ncl phenotype cannot be reliably scored in the intestine (E lineage) or the germ line; sterile hermaphrodites that had no apparent loss of the duplication in other lineages (class I) were assumed to have lost *sDp3* in P₄, the germline precursor cell, as indicated by (Ncl). Because no individuals were seen that had lost the duplication in the entire MS lineage, two Z1-Z4 mosaic animals [see (A)] were maintained at the restrictive temperature and scored for their gonadal morphology as adults. Both animals displayed normal germline anatomy and full fertility in both gonadal arms, indicating that *emb-5(+)* is not required in the distal tip cells for fertility.



not behave like null alleles at the restrictive temperature, or that *emb-5* activity perdures after the temperature shift. Alternatively, another product or pathway may be functionally redundant with *emb-5*.

The *emb-5* gene also appears to function downstream of *glp-1* in germline development. In wild-type hermaphrodites, GLP-1 is activated in the distal region of the germ line by a signal from the distal tip cell of the somatic gonad. Activation of GLP-1 promotes mitosis or inhibits meiosis or both, so that normally only distal germ nuclei divide mitotically, whereas more proximal germ nuclei undergo meiosis (3, 18). When *emb-5* mutants are shifted to the restrictive temperature after embryogenesis, they exhibit reduced germline proliferation and de-

layed or aberrant mitotic prophase (Fig. 2), consistent with a role for EMB-5 in one or more aspects of *glp-1*-mediated control of the decision between mitosis and meiosis. A number of observations support this interpretation. First, temperature-shift experiments indicate that *emb-5* activity (21), like *glp-1* activity (3), is required continuously for germline development. Second, genetic mosaic analysis indicates that *emb-5*, like *glp-1* (3), functions in the germ line (Fig. 1B). Finally, even when GLP-1 is ectopically activated, mitotic progression is impaired (Fig. 2), suggesting that *emb-5* functions downstream of *glp-1* to execute mitosis.

Taken together, the genetic and two-hybrid system data suggest that EMB-5, like Su(H), is a positive downstream effector of

LIN-12/Notch-mediated signaling. Furthermore, EMB-5, like Su(H), has been implicated in the control of gene expression. However, the molecular mechanism appears to be different. EMB-5 is a large acidic protein that is similar to the *Saccharomyces cerevisiae* Spt6p protein (22) and is also highly conserved in humans (23). Studies in yeast have suggested that Spt6p controls chromatin structure (24). The similarity of EMB-5 and Spt6p suggests that EMB-5 may coordinate chromatin changes in response to activation of LIN-12/Notch proteins, influencing the expression of genes involved in determination or execution of different developmental fates. In addition, an apparent SRC homology 2 domain seen in Spt6p (25) is conserved in the *C. elegans* and human EMB-5 proteins (21), raising the possibility that phosphorylation of tyrosine residues may regulate the activity or association of LIN-12/Notch proteins with other proteins involved in transcriptional control.

REFERENCES AND NOTES

1. D. F. Poulson, *J. Exp. Zool.* **83**, 271 (1940); R. Lehmann, F. Jimenez, U. Dietrich, J. A. Campos-Ortega, *Roux's Arch. Dev. Biol.* **192**, 62 (1983); J. R. Priess, H. Schnabel, R. Schnabel, *Cell* **51**, 601 (1987).
2. I. S. Greenwald, P. W. Sternberg, H. R. Horvitz, *Cell* **34**, 435 (1983).
3. J. Austin and J. Kimble, *ibid.* **51**, 589 (1987).
4. C. R. Coffman, P. Skoglund, W. A. Harris, C. R. Kintner, *ibid.* **73**, 659 (1993); C. P. Austin, D. E. Feldman, J. A. Ida Jr., C. L. Cepko, *Development* **121**, 3637 (1995); A. Chitnis, D. Henrique, J. Lewis, D. Ish-Horowitz, C. Kintner, *Nature* **375**, 761 (1995).
5. I. Greenwald, *Curr. Opin. Genet. Dev.* **4**, 556 (1994); S. Artavanis-Tsakonas, K. Matsuno, M. E. Fortini, *Science* **268**, 225 (1995).
6. T. Lieber, S. Kidd, E. Alcamo, V. Corbin, M. W. Young, *Genes Dev.* **7**, 1949 (1993); H. Roehl and J. Kimble, *Nature* **264**, 632 (1993); G. Struhl, K. Fitzgerald, I. Greenwald, *Cell* **74**, 331 (1993).
7. F. Schweisguth, P. Nero, J. W. Posakony, *Cell* **69**, 199 (1994).
8. S. Christensen, V. Kodoyianni, M. Bosenberg, L. Friedman, J. Kimble, *Development* **122**, 1373 (1996).
9. E. J. Lambie and J. Kimble, *ibid.* **112**, 231 (1991).
10. M. E. Fortini and S. Artavanis-Tsakonas, *Cell* **79**, 273 (1994); K. Tamura *et al.*, *Curr. Biol.* **5**, 1416 (1996).
11. F. Schweisguth, *Development* **121**, 1875 (1995).
12. S. Fields and O.-k. Song, *Nature* **340**, 245 (1989).
13. T. Durfee *et al.*, *Genes Dev.* **7**, 1 (1993).
14. R. Barstead, personal communication.
15. A total of 2.6×10^6 yeast colonies were screened. Twelve clones interacted with LIN-12 and GLP-1 but did not interact with SNF1, lamin, or FEM-1. Two of these clones contained sequences from the *emb-5* gene.
16. K. Fitzgerald, H. A. Wilkinson, I. Greenwald, *Development* **119**, 1019 (1993).
17. J. Miwa, E. Schierenberg, S. Miwa, G. von Ehrenstein, *Dev. Biol.* **76**, 160 (1980); R. Cassada, E. Isnenghi, M. Culotti, G. von Ehrenstein, *ibid.* **84**, 193 (1981).
18. J. Kimble, *ibid.* **87**, 286 (1981).
19. G. Seydoux and I. Greenwald, *Cell* **57**, 1237 (1989).
20. H. A. Wilkinson, K. Fitzgerald, I. Greenwald, *ibid.* **79**, 1187 (1994).
21. E. J. A. Hubbard, unpublished observations.
22. K. Nishiwaki, T. Sano, J. Miwa, *Mol. Gen. Genet.* **239**, 313 (1993).
23. The human sequence has been submitted to GenBank, accession number D79984, by T. Nagase *et al.*

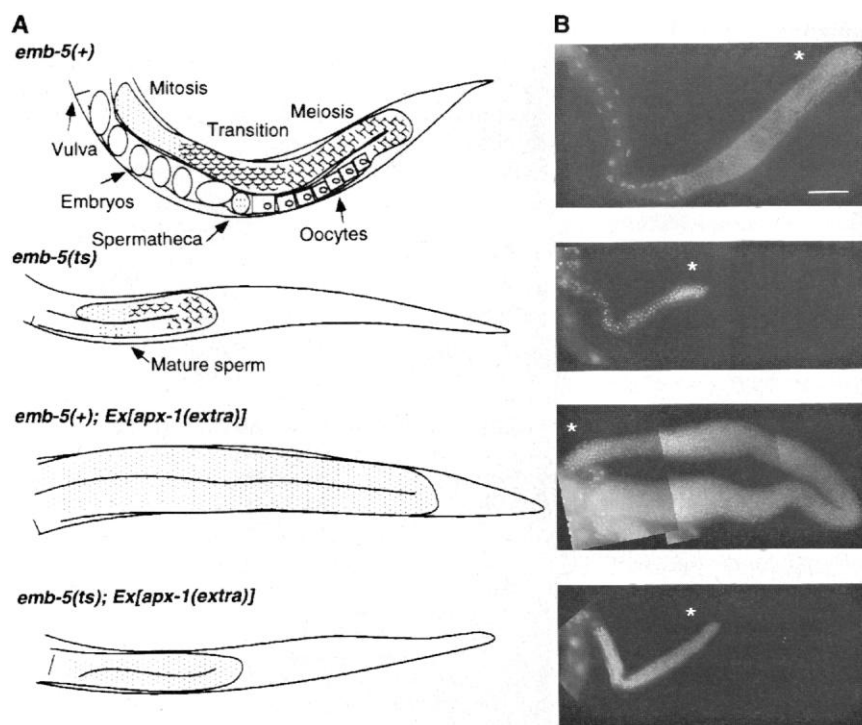


Fig. 2. The *emb-5* gene and germline proliferation. *emb-5(ts)* = *emb-5(g65)* (17) and *Ex[apx-1(extra)]* = *arEx79*, which is an extrachromosomal array that expresses the extracellular domain of APX-1 under the control of *lag-2* regulatory sequences and causes a *glp-1* gain-of-function (tumorous) phenotype (34). The *arEx79* array displays a tumorous phenotype in an otherwise wild-type background (35). Worms were synchronized by allowing adults to lay eggs for 2 to 3 hours at 15°C and transferring the eggs to 25°C for the remainder of development. Living hermaphrodites were either analyzed by Nomarski microscopy and photographed, or they were fixed and stained with 4',6-diamidino-2-phenylindole (DAPI), or both, 20 to 24 hours after the last molt. *emb-5(ts)* worms grew somewhat slower and less synchronously, reaching the last molt ~6 hours after the control strains. In addition to the germline proliferation defect, maturation of gametes in *emb-5(ts)* hermaphrodites is abnormal. In most hermaphrodites, spermatogenesis occurs (although later than in wild type), and nuclei typical of oogenesis (diakinesis arrest) are observed only rarely (20, 21). Animals carrying *arEx79* show the tumorous phenotype at a very low penetrance at 15°C (<10%) and at a high penetrance at 25°C (80%, $n = 57$ animals). One out of 36 *emb-5(ts); Ex[apx-1(extra)]* animals scored had a tumorous germ line at 25°C, and 11 of the 35 nontumorous animals were indistinguishable from *emb-5(ts)* mutants, with the remaining 24 nontumorous animals having reduced mitosis throughout the germ line and no gametogenesis, as shown here. (A) Germline anatomy, based on tracings of photomicrographs of the posterior arm of the gonad of living hermaphrodites and DAPI staining. Anterior is to the left; *emb-5(ts); Ex[apx-1(extra)]* is a ventral view, and the others are lateral views with ventral down. (B) Extruded gonads stained with DAPI, revealing the mitotic, meiotic, and differentiation state of germline nuclei. The asterisk indicates the distal end of the gonad. All photomicrographs are at the same magnification (bar = 50 μ m).

24. F. Winston and M. Carlson, *Trends Genet.* **8**, 387 (1992); A. Bortvin and F. Winston, *Science* **272**, 1473 (1996).
25. A. J. MacLennan and G. Shaw, *Trends Biochem. Sci.* **18**, 464 (1993).
26. A. M. Spence, A. R. Coulson, J. A. Hodgkin, *Cell* **60**, 981 (1990).
27. Q. Dong, unpublished observations.
28. J. H. Miller, *Experiments in Molecular Genetics* (Cold Spring Harbor Laboratory, Cold Spring Harbor, NY, 1972); L. Guarente, *Methods Enzymol.* **101**, 181 (1983).
29. M. Sundaram and I. Greenwald, *Genetics* **135**, 755 (1993).
30. I. Greenwald and G. Seydoux, *Nature* **346**, 197 (1990).
31. J. E. Sulston, E. Schierenberg, J. G. White, J. N. Thomson, *Dev. Biol.* **100**, 64 (1983); J. Kimble and D. Hirsh, *ibid.* **70**, 396 (1979).
32. E. M. Hedgecock and R. K. Herman, *Genetics* **141**, 989 (1995).
33. C. Kenyon, *Cell* **46**, 477 (1986).
34. K. Fitzgerald and I. Greenwald, *Development* **121**, 4275 (1995).
35. K. Fitzgerald, personal communication.
36. We are grateful to R. Barstead for generously providing his *C. elegans* GAD library and advice. We thank S. Elledge, G. Kalpana, S. Goff, A. Spence, J. Tu,

and X. Yang for providing plasmids, strains, and advice. We also thank E. Bucher for lessons in scoring genetic mosaics; M. Carlson, S. Hubbard, T. Schedl, P. Sherwood, and F. Winston for helpful discussion; and J. Fares, B. Grant, D. Levitan, A. Melendez, and G. Struhl for comments on the manuscript. Some of the strains used in this work were provided by the *Caenorhabditis* Genetics Center. Supported by grants from the NIH (GM37602, to I.G.) and the Damon Runyon-Walter Winchell Cancer Research Fund (to E.J.A.H.). I.G. is an Associate Investigator of the Howard Hughes Medical Institute.

1 March 1996; accepted 6 May 1996

Formation of a Transition-State Analog of the Ras GTPase Reaction by Ras·GDP, Tetrafluoroaluminate, and GTPase-Activating Proteins

Rohit Mittal,* Mohammad Reza Ahmadian,* Roger S. Goody, Alfred Wittinghofer†

Unlike the α subunits of heterotrimeric guanosine triphosphate (GTP)-binding proteins, Ras-related GTP-binding proteins have hitherto been considered not to bind or become activated by tetrafluoroaluminate (AlF_4^-). However, the product of the proto-oncogene *ras* in its guanosine diphosphate (GDP)-bound form interacted with AlF_4^- in the presence of stoichiometric amounts of either of the guanosine triphosphatase (GTPase)-activating proteins (GAPs) p120^{GAP} and neurofibromin. Neither oncogenic Ras nor a GAP mutant without catalytic activity produced such a complex. Together with the finding that the Ras-binding domain of the protein kinase c-Raf, whose binding site on Ras overlaps that of the GAPs, did not induce formation of such a complex, this result suggests that GAP and neurofibromin stabilize the transition state of the GTPase reaction of Ras.

The α subunit of heterotrimeric GTP-binding proteins (G proteins) in the GDP-bound form can be activated by the addition of the complex AlF_4^- ion. This ion is thought to mimic the terminal phosphate of GTP because the structure of the $\text{G}\alpha\cdot\text{GDP}\cdot\text{AlF}_4^-$ complex resembles that of the GTP-bound form of the protein and because binding of AlF_4^- triggers the interaction of the α subunit with downstream effectors (1). Furthermore, x-ray structure analysis of $\text{G}\alpha_{11}$ and the α subunit of transducin bound to GDP and AlF_4^- revealed that AlF_4^- activates $\text{G}\alpha\cdot\text{GDP}$ by binding with a geometry resembling that of the putative pentacovalent phosphorus intermediate, or perhaps transition state, of the GTPase mechanism (2), a possibility that had been discussed (3). In these structures, the Al ion is octahedrally coordinated with four F ligands, forming the equatorial plane, and two O ligands, supplying the apical

ligands. Because the O ligands—one contributed by a water molecule and the other by the β phosphate of GDP—correspond to the attacking nucleophile and the leaving group of the GTPase reaction, respectively, and because conserved Gln and Arg residues stabilize the complex, these structures are thought to resemble the putative pentacovalent intermediate of the GTPase reaction.

The Ras-related proteins have slow GTPase reaction rates. For Ras, this rate is 0.028 min^{-1} , which is about one-hundredth of the reaction rate of an average $\text{G}\alpha$ protein [2 to 5 min^{-1} (4)]. A number of GAPs that stimulate the GTPase reaction rate have been identified for Ras (5) and other related small G proteins (6). Four Ras-specific GAPs have been described. The p120^{GAP} and neurofibromin proteins increase the rate of GTP hydrolysis by four to five orders of magnitude at saturation (7–9). Because it seemed reasonable to assume that all G proteins have a similar mechanism of GTP hydrolysis (on the basis of structural and other similarities), it was surprising to find that Ras-related proteins do not bind AlF_4^- (10), implying that the active site of $\text{G}\alpha$ proteins in the ground state or transition state, or both, is different from that of

Ras-related proteins, although differential effects of AlF_4^- on the ribosome-stimulated GTPase reaction of elongation factor G have been reported (11).

The addition of AlF_4^- did not change the emission [or excitation (12)] spectrum of $0.1 \mu\text{M}$ Ras bound to the fluorescent GDP-analog 2'(3')-O-(N-methylanthraniloyl) GDP (mantGDP, referred to subsequently as mGDP). Such fluorescent analogs are sensitive to changes in the local structure of the protein (13, 14). Even with $5 \mu\text{M}$ Ras·mGDP and excess AlF_4^- , there was little or no change (<3%) of fluorescence (12, 15). It has been proposed that the role of GAP might be to stabilize or induce the formation of a transition state in the GTPase reaction (16), and that GAP supplies the helical domain or similar structure that exists in $\text{G}\alpha$ proteins (4) and is necessary for GTP hydrolysis (17). To test this, we added an excess of the catalytic fragment of neurofibromin NF1-333 to the solution of Ras·mGDP containing AlF_4^- (Fig. 1A). The fluorescence spectrum of mGDP revealed that the wavelength of absorption maximum changed from 448 to 430 nm and the fluorescence increase at 448 nm was 20 to 25% (and 40 to 50% at 430 nm), indicating a conformational change around the active site, which we attribute to the formation of an analog of the GTP-bound ground state or transition state of the GTPase reaction. This change was not caused by the addition of neurofibromin alone (Fig 1B); no change in fluorescence was produced after the addition of NF1-333 to Ras·mGDP, but after addition of AlF_4^- , a similar large increase of fluorescence was seen. Furthermore, the change in fluorescence was inhibited by addition of excess Ras bound to unmodified GDP, supporting the notion that complex formation is not simply due to the fluorescent label on GDP (12).

The change in fluorescence properties did not occur in the presence of catalytic amounts of neurofibromin. The effective dissociation constant (K_d) between Ras·mGDP and NF1-333 under the conditions used was 60 nM (Fig. 1C). This value is close to the K_d for the complex between

R. Mittal, M. R. Ahmadian, A. Wittinghofer, Abteilung Strukturelle Biologie, Max-Planck-Institut für Molekulare Physiologie, Rheinlanddamm 201, 44139 Dortmund, Germany.

R. S. Goody, Abteilung Physikalische Biochemie, Max-Planck-Institut für Molekulare Physiologie, Rheinlanddamm 201, 44139 Dortmund, Germany.

*These authors contributed equally to this work.

†To whom correspondence should be addressed.